

Groundwater flow in variably saturated soils characterized by stochastic fractals

Luis Guarracino * Juan E. Santos[†]

Abstract

This work presents the numerical modeling of water flow in randomly heterogeneous variably saturated soils employing a Monte Carlo simulation method. The water movement is assumed to be described by Richards equation which is solved using a mixed finite element method for the spatial discretization combined with a backward Euler and a modified Picard iteration in time. The saturated conductivity K_s and the shape parameters α_{vg} and α_{gr} in the van Genuchten and Gardner-Russo models are treated as stochastic fractal functions known as fractional Brownian motion (fBm) or fractional Gaussian noise (fGn). The mixed finite element method employed allows for the simultaneous calculation of the water content and the Buckingham-Darcy flow velocity field without performing numerical differentiation and is able to handle large variabilities and discontinuities in the stochastic parameters in Richards equation. The statistical moments of the pressure head, water content and water flow are obtained by averaging over realizations of the fractal parameters in Monte Carlo fashion. Numerical examples showing the performance of the mixed finite element method to simulate and characterize groundwater flow in highly heterogeneous soils and analyze the influence of the heterogeneities in the water flow are presented. In particular the numerical procedure is shown to be able to handle local heterogeneities in the shape parameters α_{vg} and α_{gr} used to represent local variability in the capillary relations in the unsaturated zone.

KEY WORDS: unsteady unsaturated flow, finite elements, heterogeneous soils

*CONICET, Facultad de Ciencias Astronómicas y Geofísicas, Universidad Nacional de La Plata, La Plata (1900), Argentina. E-mail: luisg@fcaglp.fcaglp.unlp.edu.ar

[†]CONICET, Facultad de Ciencias Astronómicas y Geofísicas, Universidad Nacional de La Plata, La Plata (1900), Argentina and Department of Mathematics, Purdue University, West Lafayette, IN 47907-1395, U.S.A. E-mail: santos@fcaglp.fcaglp.unlp.edu.ar, santos@math.purdue.edu

Introduction

This article concerns the numerical simulation of water flow in highly heterogeneous soils. Groundwater flow in variably saturated soils is assumed to be described by Richards equation (Richards, 1931), a highly nonlinear parabolic equation which is obtained combining the water mass conservation equation with the Buckingham-Darcy's law (Buckingham, 1907). To solve this equation, constitutive relationships of hydraulic conductivity (K) and water content (θ) versus pressure head (h) must be specified. Two of the models frequently employed in numerical simulation of water flow are the Gardner-Russo and the van Genuchten models (Gardner, 1958, Russo, 1988, van Genuchten, 1980); both of them involve the saturated hydraulic conductivity (K_s) and shape parameters denoted by α_{vg} for the van Genuchten model and α_{gr} for the Gardner-Russo model, respectively. At field scale these parameters show a high degree of spatial variability and need to be characterized using a statistical approach. For a statistical analysis of field data with measurements of the parameters α_{vg} , α_{gr} and K_s we refer to Russo and Bouton (1992) and Russo and others (1997).

It has been also observed that heterogeneities in soil properties such as the saturated conductivity K_s and the shape parameters α_{vg} and α_{gr} have logarithmic distributions and exhibit long-range correlations comparable to the size of the domain being studied. A useful tool to characterize these type of subsurface heterogeneities is to employ stochastic fractal functions, such as fractional Brownian motion (fBm) or fractional Gaussian noise (fGn). Neuman (1994), Kemblowski and Chang (1993) and Molz and Boman (1995) have reported evidence of fractal structure in saturated hydraulic conductivity distributions. In those works K_s distributions are described using fGn or fBm stochastic processes. The experimental information on the spatial variability of the shape parameters is very limited. A statistical analysis performed by Russo and Bouton (1992) and Russo and others (1997) concludes that α_{vg} and α_{gr} follow approximately lognormal distributions and show small correlation with K_s . In this work we will assume that K_s , α_{vg} and α_{gr} obey either fBm or fGn statistics and are uncorrelated.

Given that the flow equations are of stochastic nature, assuming that the statistical properties of the relevant soil properties have been determined from measurements, a Monte Carlo simulation can be employed to compute the statistical moments of the water flow. In this work we use this approach to characterize water flow in heterogeneous soils. More specifically, a set of realizations of the stochastic parameters K_s and either α_{vg} or α_{gr} with given statistical properties is synthetically generated using a spectral method. For each realization a deterministic problem associated with Richards equation is solved using a mixed finite element method for the spatial discretization combined with a backward Euler and a Picard iteration for the time discretization. After a large number of realizations the statistical moments of the pressure head, water content and flow vector are calculated. The mixed finite element procedure employed is mass conservative and can handle extremely large variabilities and discontinuities in the stochastic parameters. It also allows for the simultaneous calculation of the flow vector and the pressure head with the same degree of accuracy without having

to perform numerical differentiation, as it is the case when a standard Galerkin finite element method is employed.

The Stochastic Differential Model for Variably Saturated Flow

Let Ω be a bounded porous domain with boundary $\partial\Omega$. For $\mathbf{x} = (x, y, z)$ let $\theta = \theta(\mathbf{x})$, $h = h(\mathbf{x})$ and $\mathbf{q} = \mathbf{q}(\mathbf{x})$ denote the water content, the pressure head and the infiltration Buckingham-Darcy flow vector, respectively. It will be assumed that water flow in Ω is governed by Richards equation stated in the form

$$\frac{\partial\theta(h)}{\partial t} + \nabla \cdot \mathbf{q} = 0, \quad \mathbf{x} \in \Omega, \quad t \in I = (0, T), \quad (1a)$$

$$\mathbf{q} = -K(h)\nabla(h + z), \quad \mathbf{x} \in \Omega, \quad t \in I, \quad (1b)$$

with initial condition

$$h = h^0, \quad \mathbf{x} \in \Omega, \quad (2a)$$

and boundary conditions

$$\mathbf{q} \cdot \boldsymbol{\nu} = q^*, \quad \mathbf{x} \in \Gamma^N, \quad t \in I, \quad (3a)$$

$$h = h^*, \quad \mathbf{x} \in \Gamma^D, \quad t \in I. \quad (3b)$$

Equation (1b) is a statement of Darcy's law, with K denoting the (scalar) hydraulic conductivity, assumed to be independent of h for saturated soils but varies strongly with h in unsaturated soils; the z -axis is considered to be positive upwards. In (3a) $\boldsymbol{\nu}$ denotes the unit outer normal to $\partial\Omega$; Γ^D and Γ^N denote respectively the part of the boundary where the pressure head values h^* and the normal component of the flow q^* are being specified, with $\partial\Omega = \Gamma^D \cup \Gamma^N$, $\Gamma^D \cap \Gamma^N = \emptyset$.

To solve the differential problem (1)–(3) additional state equations relating the dependent variables θ and h are needed. In this study we consider the following water retention and hydraulic conductivity models; the van Genuchten model (van Genuchten, 1980):

$$\theta(h) = \begin{cases} \frac{\theta_s - \theta_r}{[1 + (\alpha_{vg}|h|)^n]^m} + \theta_r, & \text{for } h < 0 \\ \theta_s & \text{for } h \geq 0 \end{cases} \quad (4)$$

$$K(h) = \begin{cases} K_s \frac{\{1 - (\alpha_{vg}|h|)^{n-1}[1 + (\alpha_{vg}|h|)^n]^{-m}\}^2}{[1 + (\alpha_{vg}|h|)^n]^{m/2}} & \text{for } h < 0 \\ K_s & \text{for } h \geq 0 \end{cases} \quad (5)$$

and the Gardner-Russo model (Gardner, 1958, Russo, 1988):

$$\theta(h) = \begin{cases} (\theta_s - \theta_r) \left(\exp(0.5\alpha_{gr}h) (1 - 0.5\alpha_{gr}h) \right)^{2/(m'+2)} + \theta_r & \text{for } h < 0 \\ \theta_s & \text{for } h \geq 0 \end{cases} \quad (6)$$

$$K(h) = \begin{cases} K_s \exp(\alpha_{gr}h) & \text{for } h < 0 \\ K_s & \text{for } h \geq 0. \end{cases} \quad (7)$$

In the unsaturated zone, equation (4) (respectively (6)) states a one-to-one relation between the capillary forces and the water content (ignoring hysteresis effects), while (5) (respectively (7)) defines the effective or relative permeability of the soil (Bear, 1988). In the relations above θ_r and θ_s are the residual and saturated water contents, respectively and K_s is the saturated hydraulic conductivity. Also, n , α_{vg} and α_{gr} are shape parameters and $m = 1 - \frac{1}{n}$; m' is a parameter related to tortuosity.

According to Russo and Bouton (1992) K_s , α_{vg} and α_{gr} show a high degree of spatial variability, while the other parameters in (4)-(7) are less variable. In this article the spatial variability of K_s and α_i , $i = vg, gr$ will be modeled assuming that their spatial fluctuations are uncorrelated and can be represented by stochastic processes obeying fBm or fGn statistics. This will allow to include in the numerical model the long-range correlations of subsurface properties observed in field data measurements using the concept of self-affine fractal. The other parameters in (4)-(7) will be assumed to be constant.

Generation of Fractals using the Spectral Method

Soil heterogeneities can be modeled as fractal fBm or fGn stochastic functions having statistical self-affine structure at all scales and as a consequence having correlations over long ranges.

Recall that a self-affine stochastic fractal $f(\mathbf{x})$ in an Euclidean space of dimension E satisfies the scaling relation (Voss, 1988)

$$\gamma(\mathbf{r}) = \langle |f(\mathbf{x}) - f(\mathbf{x} + \mathbf{r})|^2 \rangle \propto |\mathbf{r}|^{2H}, \quad (8)$$

where $\langle F \rangle$ denotes the average of the random variable F , H is the Hurst exponent and $\gamma(\mathbf{r})$ is the variogram.

Following Russo and Bouton (1992) and Russo and others (1997) we assume that, for $F = K_s$ or $F = \alpha_i$, $i = vg, gr$,

$$\log F(\mathbf{x}) = \langle \log F \rangle + f(\mathbf{x}) \quad (9)$$

where the fluctuation $f(\mathbf{x})$ is a stochastic process. Further we assume that $f(\mathbf{x})$ is either a fBm or a fGn stochastic process. Self-affine stochastic fractals can be generated using

spectral techniques. Next we give a brief explanation of this approach. Recall that a fGn process is a stationary, zero mean process that can be constructed using the increments of a fBm process. Thus for a fGn process the standard spectral theory can be used to define its spectral density as the Fourier transform of the associated covariance function. On the other hand, even though a fBm process is not stationary, its spectral density can be defined using the corresponding variogram (Moltz and others, 1997).

Thus, in the sense explained above, the spectral density of a fBm/fGn process $f(\mathbf{x})$ has the form of a power law:

$$S_f(\mathbf{k}) = \frac{S_0}{|\mathbf{k}|^\beta} \quad (10)$$

where S_0 is a normalization constant, \mathbf{k} is the spatial frequency (wave number), and β is a parameter related to the Hurst exponent H and the Euclidean dimension E by the formula

$$\beta = \begin{cases} 2H + E & \text{for a fBm} \\ 2H + E - 2 & \text{for a fGn.} \end{cases} \quad (11)$$

It should be noted that in the case of a fGn realization the spectral density given by (10)–(11) is only an approximate expression because it is associated with an approximation to the covariance function of the stochastic process; a closed-form expression for the spectral density of a fGn process is not available (Moltz and others, 1997).

The value of the Hurst exponent H indicates the type of correlation and degree of persistence in fGn and fBn distributions. The range of H which is interesting and physically meaningful is $0 < H < 1$ (Moltz and others, 1997). For $H > 0.5$ there is a positive and infinite correlation both for fGn and the increments of fBm while for $H < 0.5$ this correlation is negative and infinite. When H approaches 0.5 the correlation becomes essentially zero and in this special case the classical Gaussian noise and Brownian motion are obtained. The Hurst exponent H is related to the fractal dimension D by the equation $H = 1 + E - D$ (Voss, 1988). It is important to remark that the values of H can be determined from measured data and it is also possible to discriminate fBm from fGn distributions (Liu and Moltz, 1996).

The spectral density $S_f(\mathbf{k})$ has a singular point at zero spatial frequency which corresponds to the case of an infinitely large porous media. However, the limit of the heterogeneity could not be larger than the size of the domain Ω . Therefore there is a lower frequency cutoff k_{min} which is determined by the diameter of Ω . We also consider an upper frequency cutoff k_{max} proportional to the inverse of the finite element mesh size used for the numerical simulation of water flow.

In order to obtain an expression of the normalization constant S_0 in (10) in terms of the variance σ_f^2 we integrate the spectral density (10) over the frequency domain in the range (k_{min}, k_{max}) . Then the spectral density of a fBm/fGn can be expressed as follows:

$$S_f(\mathbf{k}) = \begin{cases} \frac{C(E)\sigma_f^2(E-\beta)}{4\pi[k_{max}^{E-\beta} - k_{min}^{E-\beta}]\|\mathbf{k}\|^\beta}, & k_{max} < |\mathbf{k}| < k_{min} \\ 0, & \text{elsewhere,} \end{cases} \quad (12)$$

where $C(E) = 1, \pi^{-1}, (2\pi)^{-1}$, for $E = 1, 2, 3$, respectively.

To generate a fBm or a fGn realization we follow the ideas presented by Hassan and others (1998) and Voss (1988). First a set of uniformly distributed random numbers associated with the center of each cell of the finite element mesh is obtained using a random number generator. Then the fast Fourier transform (FFT) of this set of numbers is taken and the resulting numbers are multiplied by a transfer function proportional to $[S_f(\mathbf{k})]^{1/2}$ in the wave number space. Finally, taking the inverse FFT a set of numbers with the desired spectral density (12) is obtained.

Figure 1 shows normalized 2D realizations of fBm and fGn stochastic processes $f(\mathbf{x})$ in a square domain of side length 10 m for several fractal dimensions D and $\sigma_f^2 = .1$, with darker pixels corresponding to higher values of f . As expected, as the fractal dimension D increases we have more heterogeneity in the values of f .

Figure 2 shows the covariance $C_f(\boldsymbol{\tau})$ of the fractal fields $f(x)$ in Figure 1 computed using a discrete form of the formula

$$C_f(\boldsymbol{\tau}) = \langle (f(\mathbf{x} + \boldsymbol{\tau}) - \langle f \rangle) (f(\mathbf{x}) - \langle f \rangle) \rangle \quad (13)$$

and 500 realizations. Both for fBm and fGn distributions the correlation length diminishes as the fractal dimension D increases. In the case of a fGn, when D approaches the value 2.5 the process tends to the classical Gaussian noise characterized by having as covariance a Dirac distribution. This behavior of the covariance can be observed numerically in Figure 2.b.

In the next section we describe how to solve numerically the flow equations with stochastic coefficients K_s and α_{vg} generated as explained above.

Approximate Solution of the Flow Equations using a Mixed Finite Element Method

A Variational Formulation of the Flow Problem

The first step to approximate the solution of the flow equations is to discretize in time (1) using a backward Euler method coupled with a Picard iteration scheme as follows:

$$\frac{\theta^{n+1,i+1} - \theta^n}{\Delta t^n} + \nabla \cdot \mathbf{q}^{n+1,i+1} = 0, \quad \mathbf{x} \in \Omega, \quad (14a)$$

$$\mathbf{q}^{n+1,i+1} = -K^{n+1,i} \nabla (h^{n+1,i+1} + z), \quad \mathbf{x} \in \Omega, \quad (14b)$$

where the superscripts n and i denote time and iteration level, respectively; $\Delta t^n = t^{n+1} - t^n$ is the time step; $\theta^{n+1,i+1} = \theta(h^{n+1,i+1})$ and $K^{n+1,i} = K(h^{n+1,i})$.

Next, following Celia (1990) we expand $\theta^{n+1,i+1}$ in Taylor series with respect to h :

$$\theta^{n+1,i+1} \sim \theta^{n+1,i} + C^{n+1,i}(h^{n+1,i+1} - h^{n+1,i}), \quad (15)$$

where $C^{n+1,i} = \left(\frac{\partial \theta}{\partial h}\right)^{n+1,i}$.

Using (15) in (14) and rewriting the resulting equations in terms of the increment $\delta h^{i+1} = h^{n+1,i+1} - h^{n+1,i}$ we obtain:

$$\frac{\theta^{n+1,i} - \theta^n}{\Delta t^n} + \frac{C^{n+1,i}}{\Delta t^n} \delta h^{i+1} + \nabla \cdot \mathbf{q}^{n+1,i+1} = 0, \quad \mathbf{x} \in \Omega, \quad (16a)$$

$$\frac{\mathbf{q}^{n+1,i+1}}{K^{n+1,i}} \mathbf{q}^{n+1,i+1} + \nabla (h^{n+1,i} + \delta h^{i+1} + z) = 0, \quad \mathbf{x} \in \Omega. \quad (16b)$$

The next step will be to obtain a mixed weak formulation for (16). For this purpose it is convenient to introduce some notation. Let

$$(v, w)_D = \int_D v w \, d\Omega$$

denote the inner product in $L^2(D)$ for any subset $D \subset \Omega$. The subindex D will be omitted in the case $D = \Omega$. Also, for any $\Gamma \subset \partial\Omega$ let

$$\langle v, w \rangle_\Gamma = \int_\Gamma v w \, d\sigma$$

denote the inner product on $L^2(\Gamma)$. Set

$$\begin{aligned} V &= H(\text{div}, \Omega) = \{\mathbf{v} \in [L^2(\Omega)]^E : \nabla \cdot \mathbf{v} \in L^2(\Omega)\}, \\ V_0 &= \{\mathbf{v} \in H(\text{div}, \Omega) : \mathbf{v} \cdot \boldsymbol{\nu} = 0 \text{ on } \Gamma^N\}, \\ W &= L^2(\Omega). \end{aligned}$$

To obtain a weak formulation of (16) we multiply (16a) by $\psi \in W$ and integrate over Ω . Also, we multiply (16b) by $\mathbf{v} \in V_0$ and integrate over Ω , using integration by parts in the second term in the left-hand side of (16b) and employing the boundary condition (3b). Thus we can state a mixed weak formulation for problem (1) as follows: Assume that $(\mathbf{q}^n, h^n) \in V \times W$ are known and satisfy (3). Then, given $(\mathbf{q}^{n+1,0}, h^{n+1,0}) \in V \times W$ find $(\mathbf{q}^{n+1,i+1}, \delta h^{i+1}) \in V \times W$ such that

$$\left(\frac{\theta^{n+1,i} - \theta^n}{\Delta t^n}, \psi \right) + \left(\frac{C^{n+1,i}}{\Delta t^n} \delta h^{i+1}, \psi \right) + (\nabla \cdot \mathbf{q}^{n+1,i+1}, \psi) = 0, \quad \psi \in W, \quad (18a)$$

$$\begin{aligned} & \left(\frac{\mathbf{q}^{n+1,i+1}}{K^{n+1,i}}, \mathbf{v} \right) - (\delta h^{i+1}, \nabla \cdot \mathbf{v}) - (h^{n+1,i} + z, \nabla \cdot \mathbf{v}) \\ & + \langle h^* + z, \mathbf{v} \cdot \boldsymbol{\nu} \rangle_{\Gamma^D} = 0, \quad \mathbf{v} \in V_0, \end{aligned} \quad (18b)$$

$$\mathbf{q}^{n+1,i+1} \cdot \boldsymbol{\nu} = q^*, \quad \mathbf{x} \in \Gamma^N. \quad (18c)$$

In the next section we will define a finite element procedure for the spatial discretization of (18) in a two-dimensional rectangular domain Ω .

A Hybridized Mixed Finite Element Procedure

Let us consider the solution of the flow equations in the weak form given by (18) for the case in which the domain Ω is a rectangle. Let $\mathcal{T}^{\tilde{h}}$ be a non-overlapping partition of Ω into rectangles $\Omega_j, j = 1, \dots, n_j$ of diameter bounded by \tilde{h} :

$$\Omega = \bigcup_{j=1}^{n_j} \Omega_j; \quad \Omega_j \cap \Omega_k = \emptyset \quad j \neq k.$$

Also, set $\Gamma_{jk} = \partial\Omega_j \cap \partial\Omega_k$, $\Gamma_j = \partial\Omega_j \cap \partial\Omega$.

For $l \geq 0$ let V^l and W^l be the Raviart–Thomas–Nedelec (see Douglas and Roberts (1985) and Raviart and Thomas (1977)) mixed finite element space of index l associated with $\mathcal{T}^{\tilde{h}}$, i.e.,

$$\begin{aligned} V^l &= \{ \mathbf{v} \in H(\text{div}, \Omega) : \mathbf{v}|_{\Omega_j} \in P_{l+1,l} \times P_{l,l+1} \}, \\ V_0^l &= \{ \mathbf{v} \in V^l \text{ and } \mathbf{v} \cdot \boldsymbol{\nu} = 0 \text{ on } \Gamma^N \}, \\ W^l &= \{ \psi \in L^2(\Omega) : \psi|_{\Omega_j} \in P_l \}, \end{aligned} \quad (19a)$$

where P_m denote the polynomials of total degree not greater than m and $P_{m,n}$ denotes the polynomials of degree not greater than m in the x-variable and not greater than n in the z-variable. In order that elements $\mathbf{v} \in V^l$ be in $H(\text{div}, \Omega)$ their normal components must be continuous across the inter-element boundaries Γ_{jk} . The mixed finite element procedure for the approximate solution of the flow problem is defined as the discrete analogue of (18) by replacing V , V_0 and W by V^l , V_0^l and W^l , respectively; the associated algebraic problem consists of the solution of a linear system of equations for the coefficients of the expansion of the flow vector and pressure head in a basis of $V_0^l \times W^l$. Following Arnold and Brezzi (1985), we will simplify the algebraic form associated with the mixed method by eliminating the constrain imposing the continuity

of the normal components of the flow vector across the interior boundaries and enforcing the required continuity instead using a Lagrange multiplier. Thus we introduce a space of Lagrange multipliers Λ^l which elements λ are associated with the potential $h + z$ at the inter-element boundaries Γ_{jk} . Let

$$\begin{aligned}\Lambda^l &= \{\lambda : \lambda|_{\Gamma_{jk}} = \lambda_{jk} \in P_l(\Gamma_{jk})\}, \\ V_{-1}^l &= \{\mathbf{v} \in L^2(\Omega) : \mathbf{v}|_{\Omega_j} \in P_{l+1,l} \times P_{l,l+1}\}, \\ V_{0,-1}^l &= \{\mathbf{v} \in V_{-1}^l \text{ and } \mathbf{v} \cdot \boldsymbol{\nu} = 0 \text{ on } \Gamma^N\}.\end{aligned}\tag{20a}$$

Next, to obtain a hybridized form of the mixed method we multiply (16a) by $\psi \in W^l$ and integrate over Ω . Also, we multiply (16b) by $\mathbf{v} \in V_{0,-1}^l$ and integrate over Ω , using integration by parts at the element level in the second term in the left-hand side of (16b) and the fact that the Lagrange multipliers are associated with the potential $h + z$ on Γ_{jk} . Note that we can not use integration by parts globally in Ω because functions in $V_{0,-1}^l$ do not have divergence defined globally in $L^2(\Omega)$.

Thus the hybridized mixed finite element procedure is defined in the following fashion : Let $(\mathbf{Q}^n, H^n, \lambda^n) \in V_{-1}^l \times W^l \times \Lambda^l$ be given and such that (\mathbf{Q}^n, H^n) satisfies (3). Then, given $(\mathbf{Q}^{n+1,0}, H^{n+1,0}, \lambda^{n+1,0}) \in V_{-1}^l \times W^l \times \Lambda^l$, find $(\mathbf{Q}^{n+1,i+1}, H^{n+1,i+1}, \lambda^{n+1,i+1}) \in V_{-1}^l \times W^l \times \Lambda^l$ such that

$$\begin{aligned}\left(\frac{\Theta^{n+1,i} - \Theta^n}{\Delta t^n}, \psi\right) + \left(\frac{C^{n+1,i}}{\Delta t^n} \delta H^{h,i+1}, \psi\right) \\ + \sum_j (\nabla \cdot \mathbf{Q}^{n+1,i+1}, \psi)_{\Omega_j} = 0, \quad \psi \in W^l,\end{aligned}\tag{21a}$$

$$\left(\frac{\mathbf{Q}^{n+1,i+1}}{K^{n+1,i}}, \mathbf{v}\right) - \sum_j (\delta H^{i+1}, \nabla \cdot \mathbf{v})_{\Omega_j} - \sum_j (H^{n+1,i} + z, \nabla \cdot \mathbf{v})_{\Omega_j}\tag{21b}$$

$$+ \langle h^* + z, \mathbf{v} \cdot \boldsymbol{\nu} \rangle_{\Gamma^D} + \sum_{jk} \langle \lambda_{jk}^{n+1,i+1}, \mathbf{v} \cdot \boldsymbol{\nu} \rangle_{\Gamma_{jk}} = 0, \quad \mathbf{v} \in V_{0,-1}^l,$$

$$\mathbf{Q}^{n+1,i+1} \cdot \boldsymbol{\nu} = Q^*, \quad \mathbf{x} \in \Gamma^N,\tag{21c}$$

$$\sum_{jk} \langle \mu, \mathbf{Q}^{n+1,i+1} \cdot \boldsymbol{\nu} \rangle_{\Gamma_{jk}} = 0, \quad \mu \in \Lambda^l.\tag{21d}$$

Note that equation (21d) is equivalent to the condition that $\mathbf{Q}^{n+1,i+1} \in H(\text{div}, \Omega)$. In (21c) Q^* is an approximation to q^* defined locally on Γ^N as follows:

$$Q^*|_{\Gamma_j} = Q_j^* \quad \text{for } \Gamma_j \subset \Gamma^N,$$

where Q_j^* is determined by the relation

$$\langle Q_j^* - q^*, \varphi \rangle_{\Gamma_j} = 0, \quad \varphi \in P_l(\Omega_j).$$

Set $h^{n+1} \equiv h^{n+1,\infty}$, with $h^{n+1,\infty}$ denoting the value of the pressure head after convergence of the Picard iteration (18) has been achieved for a prescribed tolerance, and define $\mathbf{q}^{n+1}, H^{n+1}, \mathbf{Q}^{n+1}$ in a similar fashion. Then using the fact that a backward Euler scheme is first order correct in time, the results given in Douglas and Roberts (1985) imply that

$$\|H^{n+1} - h^{n+1}\|_{L^2(\Omega)} \propto \tilde{h}^{l+1} + \max_n \Delta t^n,$$

$$\|\mathbf{Q}^{n+1} - \mathbf{q}^{n+1}\|_{L^2(\Omega)} \propto \tilde{h}^{l+1} + \max_n \Delta t^n.$$

The method (21) was implemented for the lowest-order index case $l = 0$. The corresponding degrees of freedom are the values of the pressure head H^{n+1} at the center of the rectangles Ω_j and the values of the normal component of the water flow vector \mathbf{Q}^{n+1} and the Lagrange multipliers λ^{n+1} at the mid points of the sides of Ω_j . Also, after employing a trapezoidal quadrature rule to compute the first term in the left-hand side of (21b), we obtain a linear system for the values of the pressure head H^n at the mid points of the rectangles Ω_j , so that in the case $l = 0$ the procedure (21) may be regarded as a cell-centered finite difference scheme. We also implemented a dynamic time step control which significantly improved the CPU efficiency. The time step is increased or decreased depending of the number of iterations required for the Picard iteration to converge. The automatic time adjustment is stopped when the time step becomes either smaller or greater than preselected minimum and maximum step sizes. The numerical procedure just described was validated in Guarracino (2001) by comparison with analytical solutions presented by Ross and Parlange (1994) and Strivastava and Yeh (1991). In the next section we show numerical examples with the implementation of this procedure to simulate flow in highly heterogeneous soils with soil parameters obeying either fBm or fGn statistics.

Monte Carlo Simulations of Water Flow

The Monte Carlo simulation method consists in solving Richards equation for a large number of realizations of the stochastic processes K_s and α_i , $i = vg$ or $i = gr$. We computed the variance of the pressure head, water content and the water flow at the cell centers of the finite element mesh and observed that the variance values stabilized after a certain number of realizations. Thus we adopted the criteria of stopping the Monte Carlo simulation when a global measure of the variance of the pressure head, water content and the water flow over the domain Ω have converged to asymptotic values within a small tolerance. More specifically, for $s = h, \theta, q_x, q_z$ we defined the spatial average of the variance of s as follows:

$$\|\sigma_s^{2,m}\| = \left[\frac{1}{n_j} \sum_{j=1}^{n_j} \left(\sigma_{s_j}^{2,m} \right)^2 \right]^{1/2} \quad (22)$$

where $\sigma_{s_j}^{2,m}$ denotes the variance of s computed at the center of the subdomain Ω_j after m -realizations. Thus, setting $\Delta\sigma_s^{2,m} = \|\sigma_s^{2,m} - \sigma_s^{2,m-1}\|$, we consider that the Monte Carlo simulation converges when for a given ϵ sufficiently small we have that

$$\frac{\Delta\sigma_s^{2,m}}{\Delta\sigma_s^{2,4}} \leq \epsilon. \quad (23)$$

Once the convergence has been achieved we proceed to compute the statistical moments of the variables of interest. For the stochastic variable s we computed the mean value $\langle s_j \rangle^N$ and variance $\sigma_{s_j}^{2,N}$ associated with the center of the subdomain Ω_j and the covariance $C_{s_j s_k}^N$ associated with the centers of the subdomains Ω_j and Ω_k after N Monte Carlo realizations using the relations

$$\langle s_j \rangle^N = \langle s_j \rangle = \frac{1}{N} \sum_{m=1}^N s_j^m, \quad (24a)$$

$$\sigma_{s_j}^{2,N} = \frac{1}{N-1} \sum_{m=1}^N (s_j^m - \langle s_j \rangle)^2 = \frac{N}{N-1} [\langle (s_j)^2 \rangle - (\langle s_j \rangle)^2], \quad (24b)$$

$$C_{s_j s_k}^N = \frac{1}{N} \sum_{m=1}^N (s_j - \langle s_j \rangle)(s_k - \langle s_k \rangle) = \langle s_j s_k \rangle - \langle s_j \rangle \langle s_k \rangle. \quad (24c)$$

To illustrate the use of the Monte Carlo method we will consider the water flow in a rectangular domain Ω of 12 m in the horizontal direction by 8 m in the vertical direction. The water table is considered to be horizontal and located at a depth of 6 m. We consider a hydrostatic initial condition ($\mathbf{q} = 0$). At the upper boundary of Ω (surface, $z = 8$ m) we specify a constant infiltration rate of 12 mm/d over an interval of size 6 m at the center of this boundary. At the bottom ($z = 0$) and lateral boundaries of Ω we specified the values of the pressure head corresponding to the hydrostatic state. For the constitutive relations we chose the van Genuchten model with parameter values corresponding to a sandy loam obtained by Carsel and Parrish (1988) and given in Table 1, where we also give the values for the variance of K_s and α_{vg} used for the generation of the corresponding fractal fields.

For the spatial discretization we employed a uniform mesh of 48×32 subdomains. The automatic time step adjustment described above was implemented with maximum and minimum values of 1 hour and 6 seconds, respectively. The total simulation time for each realization was 15 days in order to develop an infiltration front in the upper part of the domain. The experiments were run in the computer IBM SP2 at Purdue University used as a single processor machine, with an average simulation time for each realization of 5 minutes. We run a total of 1000 Monte Carlo simulations and then computed all statistical moments at $T = 15$ days as explained before.

Figures 3 and 4 display realizations of the fractal conductivity field K_s corresponding to the values in Table 1 for fBm and fGn distributions, respectively, and fractal dimension $D=2.2$. The conductivity values show a high degree of heterogeneity, with

an order of magnitude variation between minimum and maximum values. Also, as expected, we observe more persistence in the fBm than in the fGn realization of K_s .

In Figures 5 and 6 we show the water content θ at $T = 15$ days for a single realization of K_s and α_{vg} for fBm and fGn distributions and fractal dimension $D = 2.2$. In both cases it is clearly observed the effects of the local heterogeneities on the water content distribution in the soil.

Figures 7 and 8 display the corresponding flow fields for the same single realization, where we can observe the water motion where the infiltration is taking place (upper part of the domain), while in the rest of the domain the flow is negligible.

In Figures 9 and 10 we show the average and variance σ_θ^2 of the water content θ at $T = 15$ days for the case of an fBm distribution and fractal dimension $D = 2.2$. Notice that σ_θ^2 vanishes in the saturated zone since in this region $\theta(h) = \theta_s$. The variance σ_θ^2 attains its maximum values close to the water table, in the region known as the capillary fringe. The variance also shows an increase along the infiltration front.

Figures 11 and 12 display the average value and the variance of the vertical component q_z of the flow vector. It can be observed that the maximum values of the variance $\sigma_{q_z}^2$ are located in the region where the infiltration is taking place.

Next we present an experiment that illustrates the stabilization of the variance mentioned above. To show this behavior we selected somehow arbitrarily four points as follows: $P_1 = (5.875, 6.625)$ in the infiltration region, $P_2 = (5.875, 6.125)$ approximately on the infiltration front, $P_3 = (5.875, 5.625)$ about 0.5 m below the infiltration front and $P_4 = (5.875, 2.125)$ above the water table. Figure 13 shows the variance σ_θ^2 of the water content assuming fBm distributions and $D = 2.2$ at time $T = 15$ days; it can be observed that the variance values stabilizes at the four points after 500 realizations. The same stabilization effect was observed for the other variables (h , q_x , q_z) using either the van Genuchten or the Gardner-Russo model, for fGn distributions and other fractal dimensions.

Next we analyze the behavior of the variance of the water content σ_θ^2 for the case in which, for each realization of the stochastic permeability field K_s , the parameter α_{vg} is a random constant over the domain Ω with average value 0.075 cm^{-1} and variance of $\ln(\alpha_{vg})$ equal to 0.10. This simplification (that contradicts experimental evidence) is done by Tartakovsky and others (1999) to study stochastic unsaturated flow using a Kirchhoff transformation. Figure 14 shows values of σ_θ^2 at the point P_1 as function of the number of Monte Carlo realizations for the case in which α_{vg} is either a constant over the domain Ω for each realization or a fBm process with $D = 2.2$. As expected, σ_θ^2 stabilizes much earlier in the former case. In particular, this Figure shows that the numerical procedure is robust and capable to handle local heterogeneities in the parameter α_{vg} , used to represent local variability of the capillary relations in the unsaturated zone (c.f. (4)-(6)).

Figure 15 shows a log-log plot of the increments $\Delta\sigma_s^{2,m}$ as function of the number of realizations m for $s = \theta, h, q_x, q_z$. The Figure shows that to obtain one order of magnitude in the error reduction in the calculation of the moments we need to increase in one order of magnitude the number of Monte Carlo realizations.

Finally, the covariance of the vertical component of the flow q_z in the horizontal and vertical directions is displayed in Figures 16 and 17, respectively, at the points P_1, P_2 and P_3 . It can be observed that the covariances depend on the point and the direction at which are being calculated, showing numerically that the flow field is not stationary. Also note that in Figure 17 the covariance tends to zero near $z = 8$ m, i.e., close to the surface. This is due to the fact that the boundary condition imposed at such boundary is deterministic and of Neumann type; below the infiltration front the covariance also vanishes because the initial condition corresponds to the hydrostatic case ($\mathbf{q} = 0$).

Conclusions

In the present paper a robust, mass conservative mixed finite element method was used in Monte Carlo fashion to simulate unsteady variably saturated groundwater flow in highly heterogeneous soils. The saturated conductivity K_s and the shape parameters α_{vg} and α_{gr} in the van Genuchten and Gardner-Russo models were assumed to be stochastic fractal functions obeying either fBm or fGn statistics. The numerical procedure is able to compute simultaneously the water flow and the pressure head with equal accuracy without having to perform numerical differentiation or local smoothing of the stochastic coefficients in Richards equations. A parametric analysis of the model was performed, analyzing the sensitivity of the dependent variables with respect to representative statistical parameters such as the fractal dimension and the distribution type (fBm/fGn) of the soil being modeled. The statistical moments of the water content, pressure head and water flow were computed by averaging over realizations of the fractal parameters characterizing the soil heterogeneity. A new practical criteria to stop the Monte Carlo simulation based on the stabilization of the variances of the computed variables is also presented.

Acknowledgements

This work has been funded by the Agencia Nacional de Promoción Científica y Tecnológica Argentina (contract BID 802/0C-AR) and CONICET, Argentina, PIP 0363/98.

References

- [1] D. N. Arnold and F. Brezzi, 1985, *Mixed and nonconforming finite element methods: implementation, postprocessing and error estimates*, R.A.I.R.O. Modélisation, Mathématique et Analyse Numérique, 19, p. 7-32.
- [2] J. Bear, 1988, *Dynamics of Fluids in Porous Media*, Dover, New York, 764 p.
- [3] R. F. Carsel and R. S. Parrish, 1988, *Developing joint probability distributions of soil water characteristics*, Water Resources Research, 24, p. 755-769.
- [4] M. A. Celia, E. T. Bouloutas, and R. L. Zarba, 1990, *A general mass-conservative numerical solution for the unsaturated flow equation*, Water Resources Research, 26, p. 1483-1496.
- [5] E. Buckingham, 1907, *Studies on the movement of soil moisture*, Bureau of Soil Bulletin 38, Washington, D. C., U. S. Department of Agriculture.
- [6] J. Douglas, Jr., and J. E. Roberts, 1985, *Global estimates for mixed methods for second order elliptic equations*, Mathematics of Computation, 44, p. 39-52.
- [7] W. R. Gardner, 1958, *Some steady state solutions of unsaturated moisture flow equations with application to evaporation from a water table*, Soil Sci., 85, p. 228-232.
- [8] L. Guarracino, 2001, *Modelado numérico del flujo de aguas subterráneas y transporte de solutos en medios porosos heterogéneos*, PhD thesis, Facultad de Cs. Astr. y Geof., Universidad Nacional de La Plata, La Plata, Argentina, 118 p.
- [9] A. Hassan, J. H. Cushman and J. W. Delleur, 1998, *A Monte Carlo assessment of Eulerian flow and transport perturbation models*, Water Resources Research, 34, p. 1143-1163.
- [10] M. W. Kemblowski and C. M. Chang, 1993, *Infiltration in soils with fractal permeability distribution*, Ground Water, 31, p. 187-192.
- [11] H. H. Liu and F. J. Moltz, 1996, *Discrimination of fractional Brownian movement and fractional Gaussian noise structures in permeability and related property distributions with range analyses*, Water Resour. Res., 32, p. 2601-2605.
- [12] F. J. Moltz and G. K. Boman, 1995, *Further evidence of fractal structure in hydraulic conductivity distributions*, Geophys. Res. Letters, 22, p. 2545-2548.
- [13] Moltz, F. J., H. H. Liu and J. Szulga, 1997, *Fractional Brownian motion and fractional Gaussian noise in subsurface hydrology: A review, presentation of fundamental properties and extensions*, Water Resour. Res., 33 (10), p. 2273-2286.

- [14] S. P. Neuman, 1994, *Generalized scaling of permeabilities: Validation and effect of support scale*, Geophys. Res. Letters, 21, p. 349-352.
- [15] P. A. Raviart, and J. M. Thomas, 1977, *A mixed finite element method for second order elliptic problems*, Mathematical Aspects of the Finite Element Method, Lecture Notes in Mathematics, 606, p. 292-315.
- [16] L. Richards, 1931, *Capillary conduction of liquids through porous mediums*, Physics, 1, p. 318-333.
- [17] P. J. Ross and J. Y. Parlange, 1994, *Comparing exact and numerical solutions for Richards' equation for one-dimensional infiltration and drainage*, Soil Science, 157, p. 341-344.
- [18] D. Russo, 1988, *Determining soil hydraulic properties by parameter estimation: On the selection of a model for the hydraulic properties*, Water Resour. Res., 24, p. 453-459.
- [19] D. Russo and M. Bouton, 1992, *Statistical Analysis of Spatial Variability in Unsaturated Flow Parameters*, Water Resour. Res., 28, p. 1911-1925.
- [20] D. Russo, I. Russo and A. Laufer, 1997, *On the spatial variability of parameters of the unsaturated hydraulic conductivity*, Water Resour. Res., 33, p. 945-956.
- [21] R. Strivastava and T. C. Jim Yeh, 1991, *Analytical solutions for one-dimensional, transient infiltration toward the water table in homogeneous and layered soils*, Water Resour. Res., 27, p. 753-762.
- [22] D. M. Tartakovsky and S. P. Neuman and Z. Lu, 1999, *Conditional stochastic averaging of steady state unsaturated flow by means of Kirchhoff transformation*, Water Resour. Res., 35, p. 731-745.
- [23] M. T. van Genuchten, 1980, *A closed-form equation for predicting the hydraulic conductivity of unsaturated soils*, Soil Sci. Soc. Am. J., 44, p. 892-898.
- [24] R. F. Voss, 1988, *Fractals in nature: From characterization to simulation*, The Science of Fractal Images, edited by H. Peitgen and D. Saupe, Springer-Verlag, p. 21-69.

Figure Captions

Figure 1: Realizations of fBm distributions for a) $D = 2.05$, b) $D = 2.25$, c) $D = 2.45$ and fGn distributions for e) $D = 2.05$, f) $D = 2.25$, g) $D = 2.45$.

Figure 2: Covariance functions of fBm and fGn distributions for $D = 2.05, 2.25$ and 2.45 .

Figure 3: Realization of a permeability field K_s generated using fBm distributions.

Figure 4: Realization of a permeability field K_s generated using fGn distributions.

Figure 5: Realization of a water content field generated using fBm distributions.

Figure 6: Realization of a water content field generated using fGn distributions.

Figure 7: Realization of a water flow field generated using fBm distributions.

Figure 8: Realization of a water flow field generated using fGn distributions.

Figure 9: Mean water content field for fBm distributions and 1000 Monte Carlo realizations.

Figure 10: Variance of water content field for fBm distributions and 1000 Monte Carlo realizations.

Figure 11: Mean q_z field for fBm distributions and 1000 Monte Carlo realizations.

Figure 12: Variance of q_z for fBm distributions and 1000 Monte Carlo realizations.

Figure 13: Stabilization of the water content variance at P_1, P_2, P_3 and P_4 .

Figure 14: Influence of the parameter α_{vg} on the stabilization of the water content variance at P_1 .

Figure 15: Convergence of the Monte Carlo simulation method.

Figure 16: Covariance of q_z in the x -direction computed at the points P_1, P_2 and P_3 .

Figure 17: Covariance of q_z in the z -direction computed at the points P_1, P_2 and P_3 .

	K_s (cm/s)	α_{vg} (cm ⁻¹)	n	1.89
$\langle F \rangle$	$1.22 \cdot 10^{-3}$	0.075	θ_s	0.41
σ_f^2	0.2	0.10	θ_r	0.065

Table 1: Parameters of the van Genuchten model.

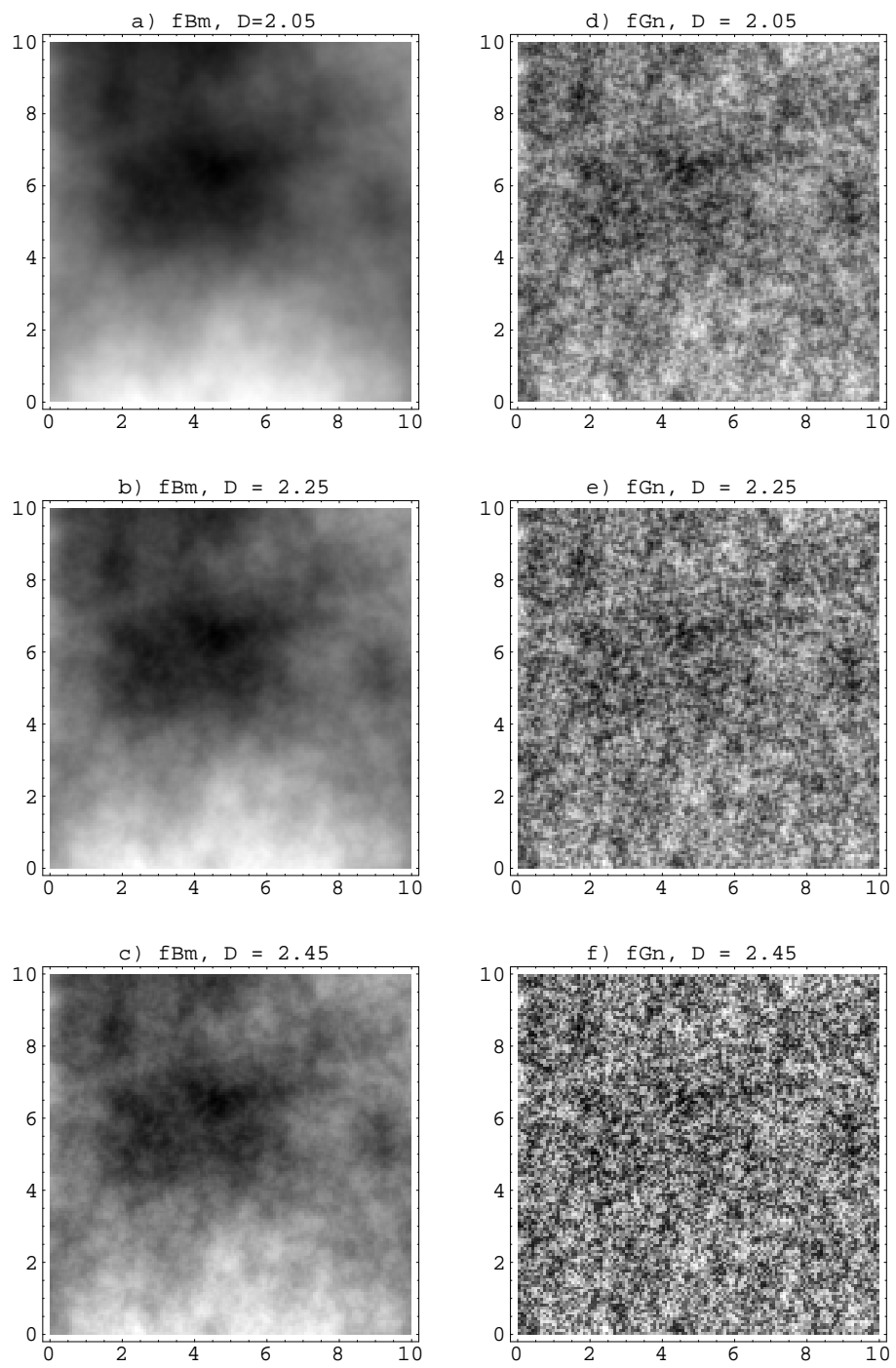


Figure 1

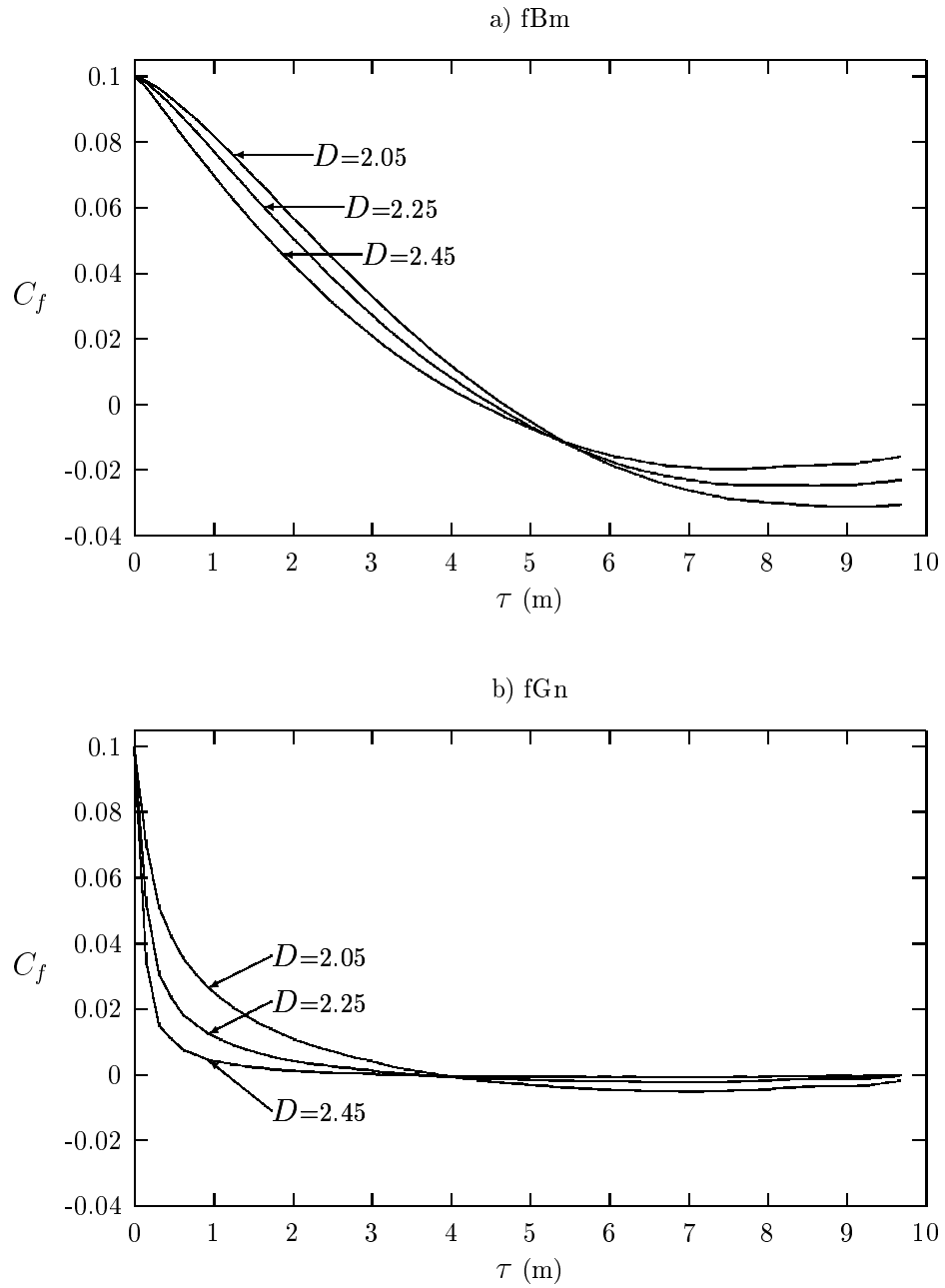


Figure 2

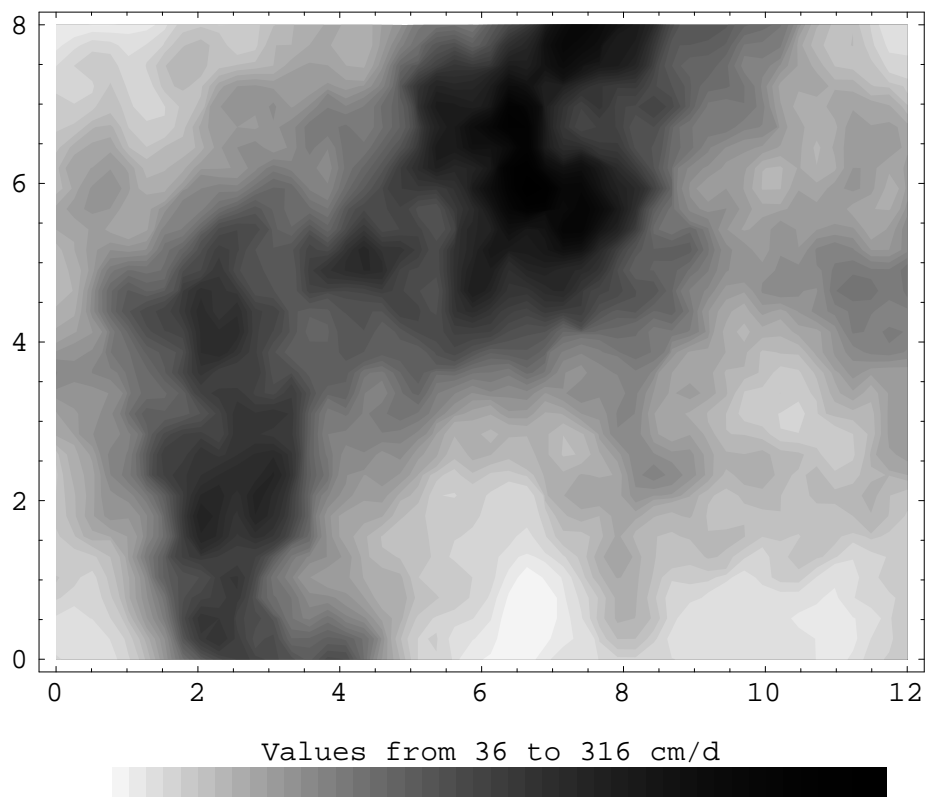


Figure 3

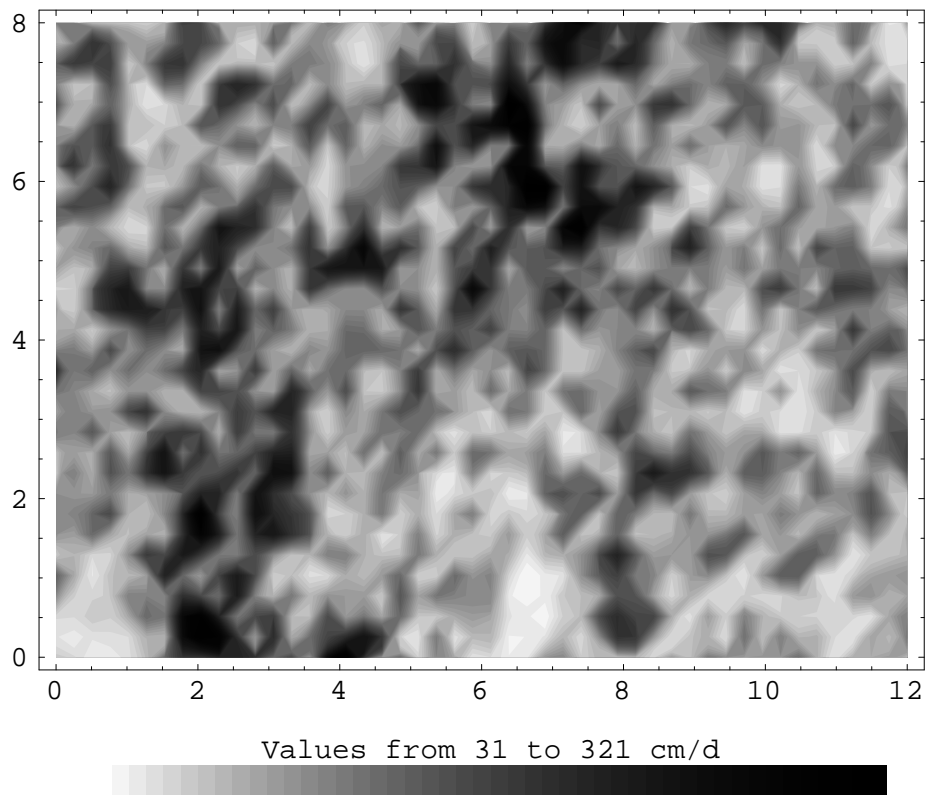


Figure 4

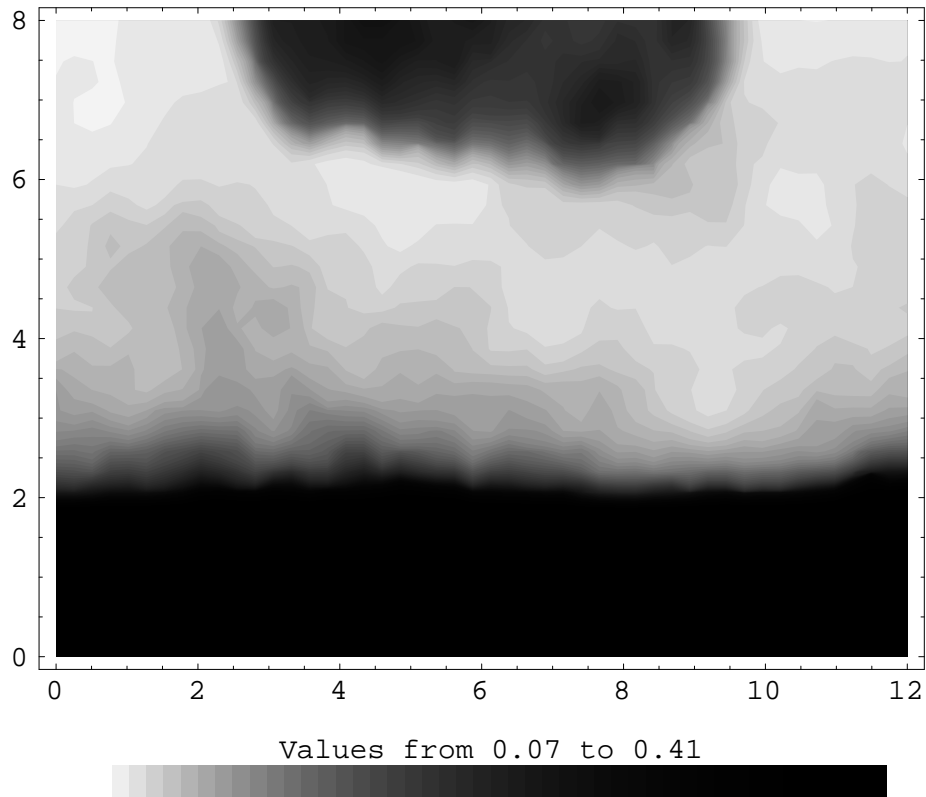


Figure 5

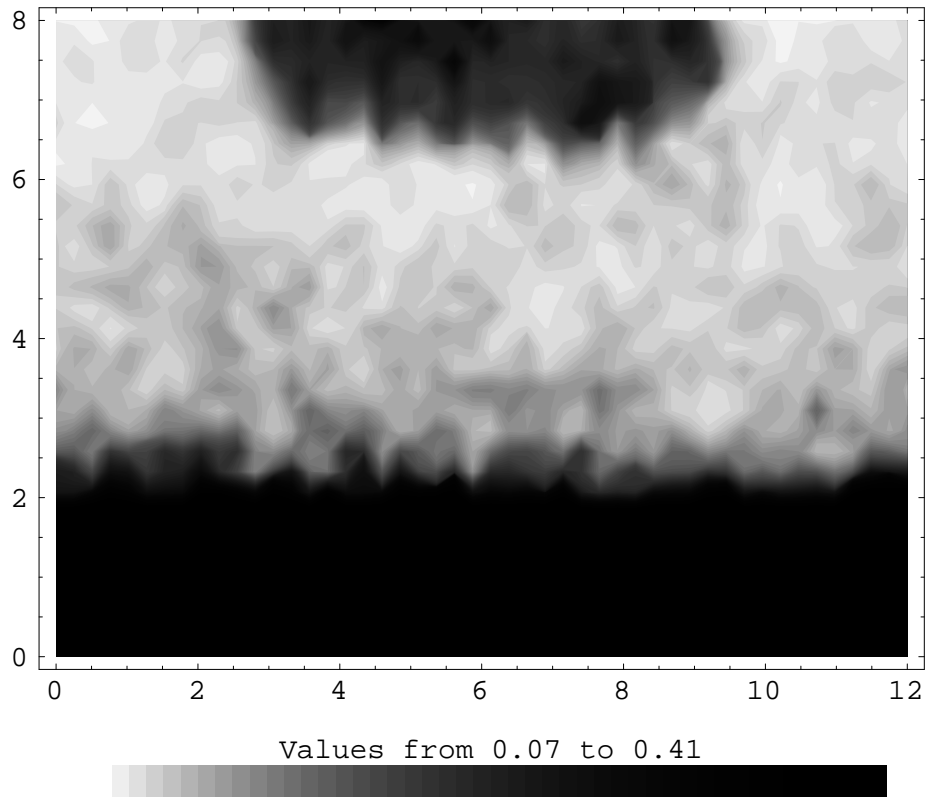


Figure 6

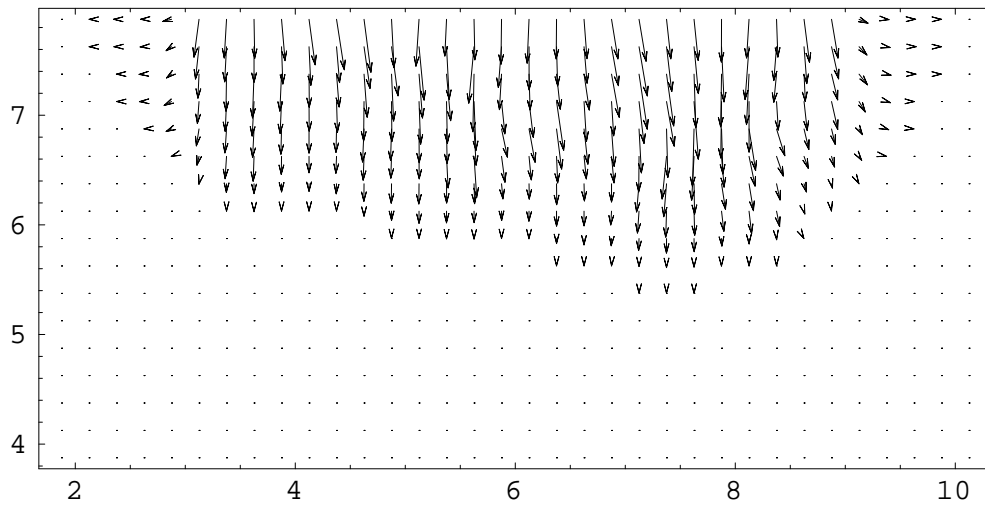


Figure 7

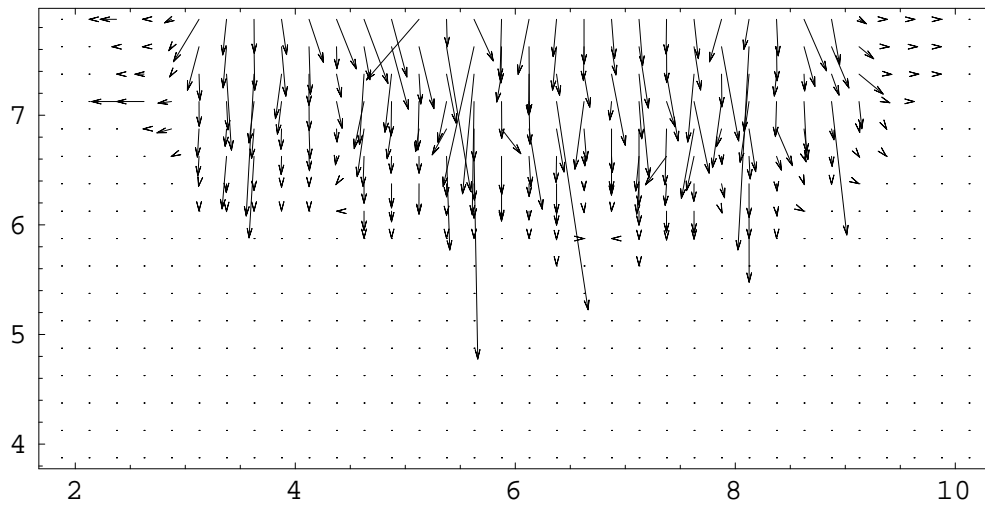


Figure 8

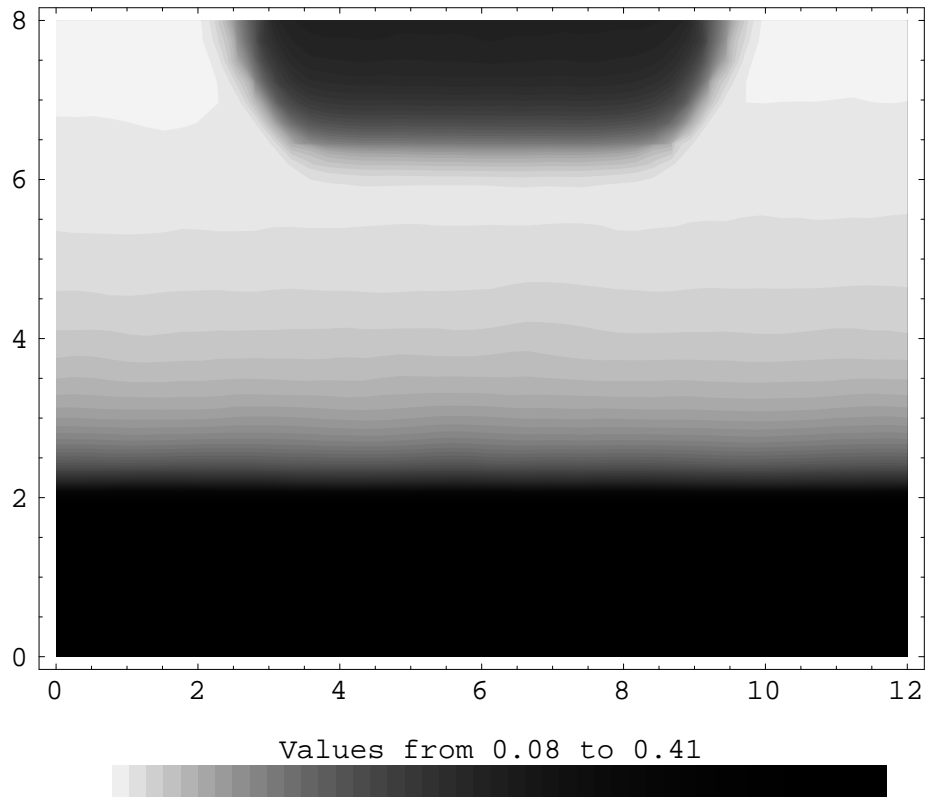


Figure 9

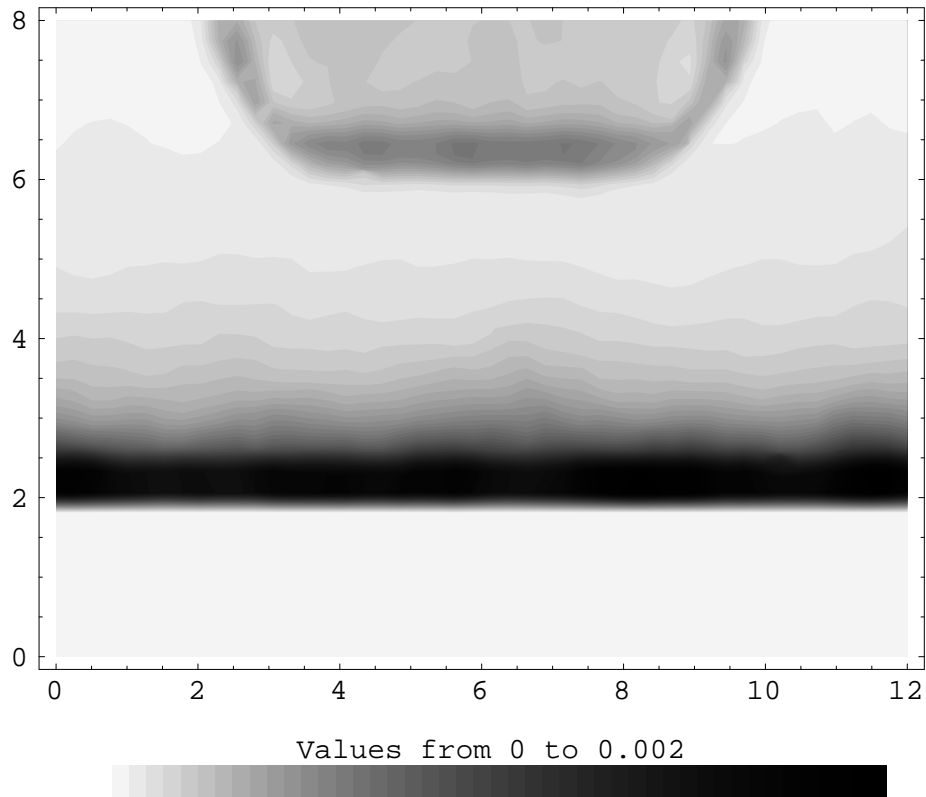


Figure 10

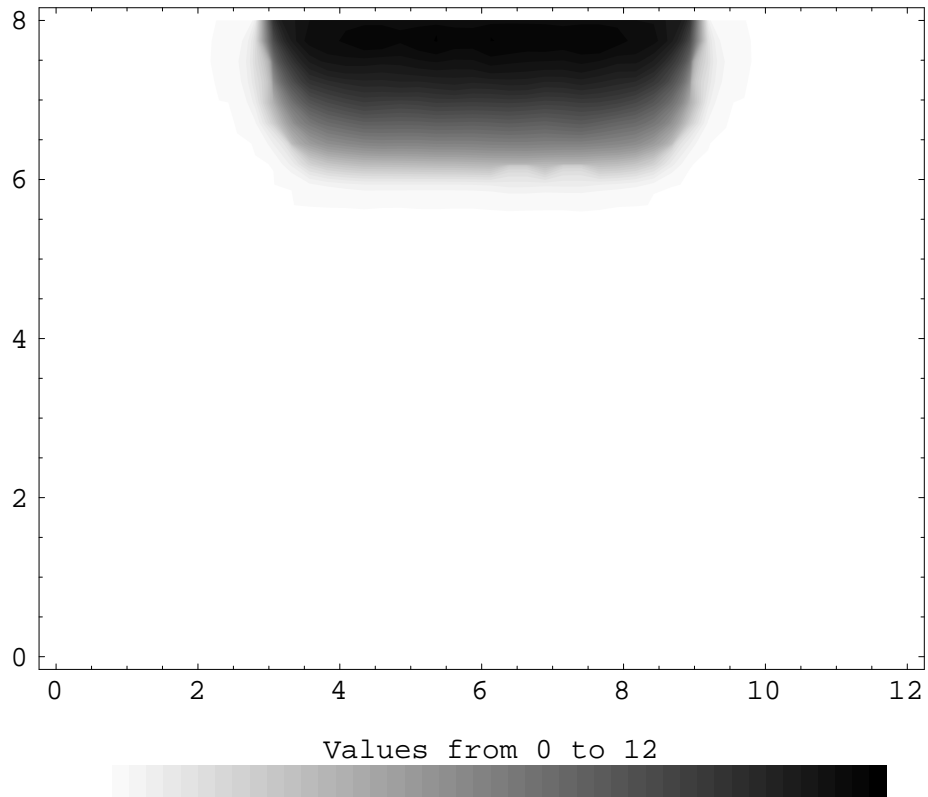


Figure 11

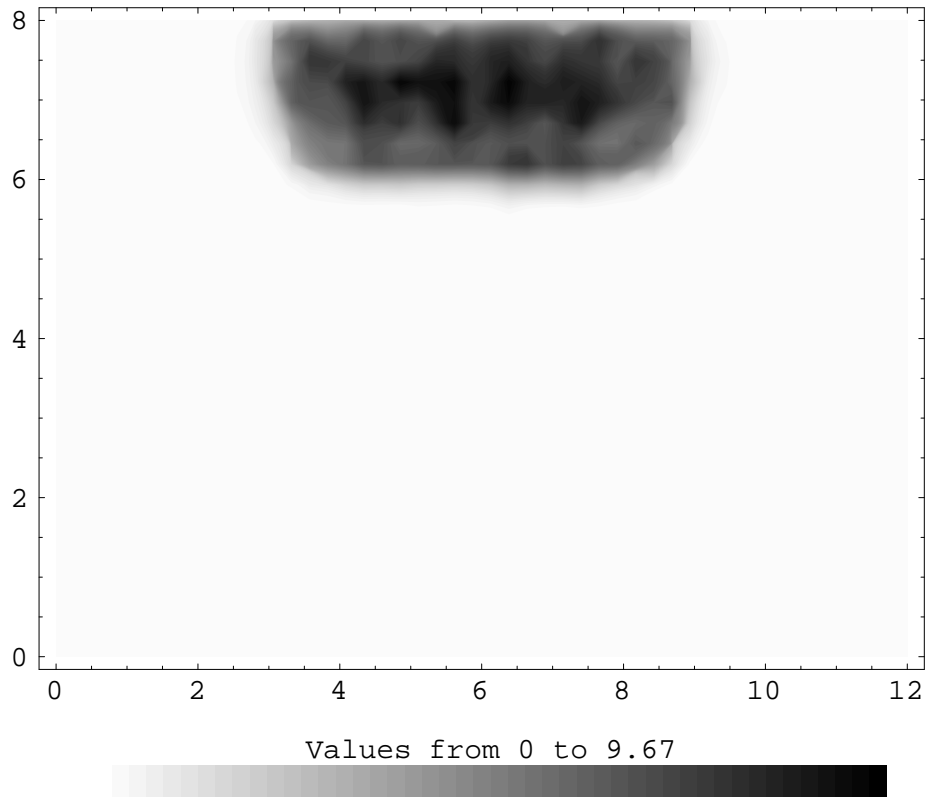


Figure 12

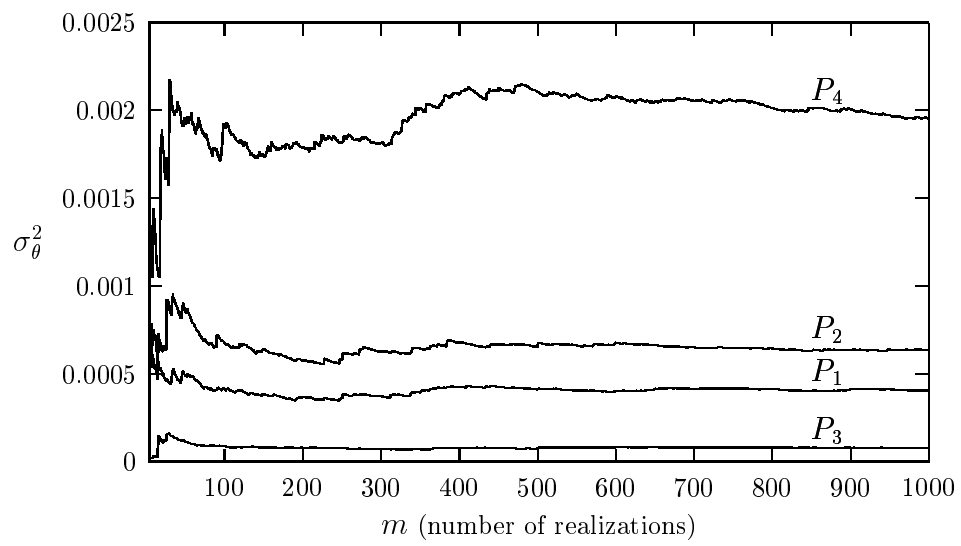


Figure 13

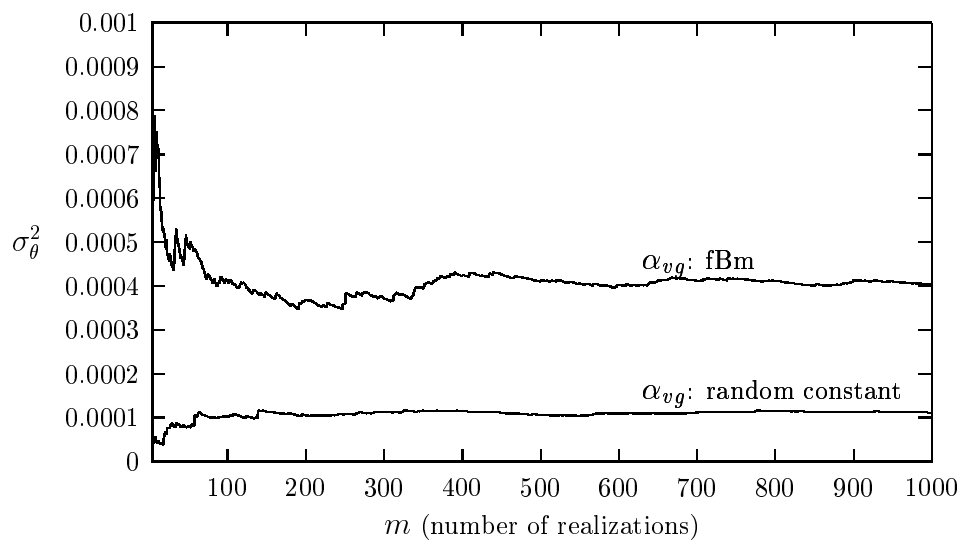


Figure 14

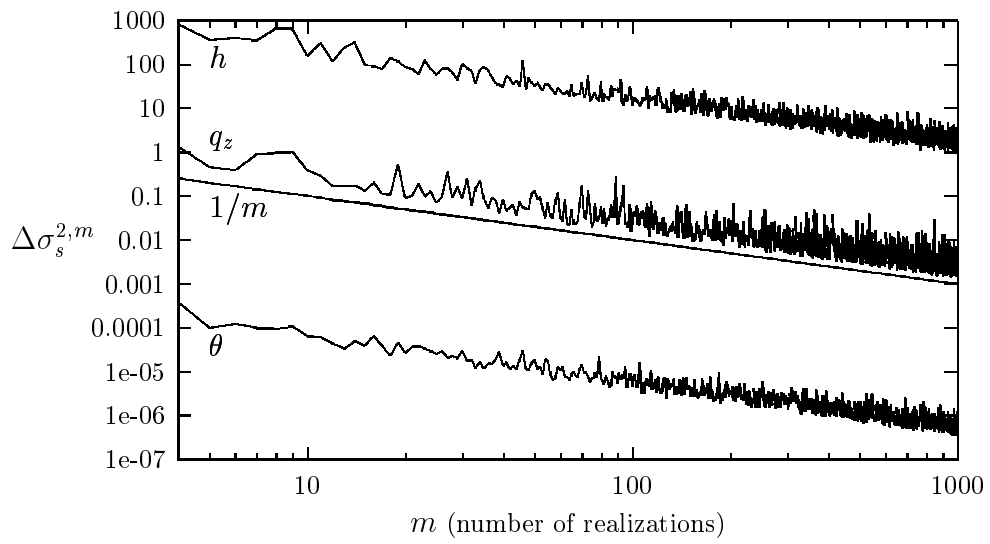


Figure 15

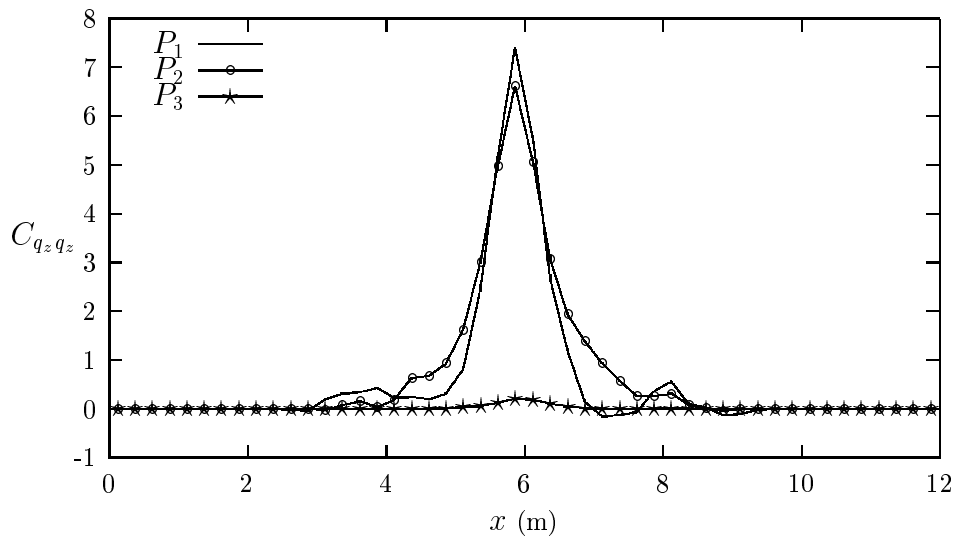


Figure 16

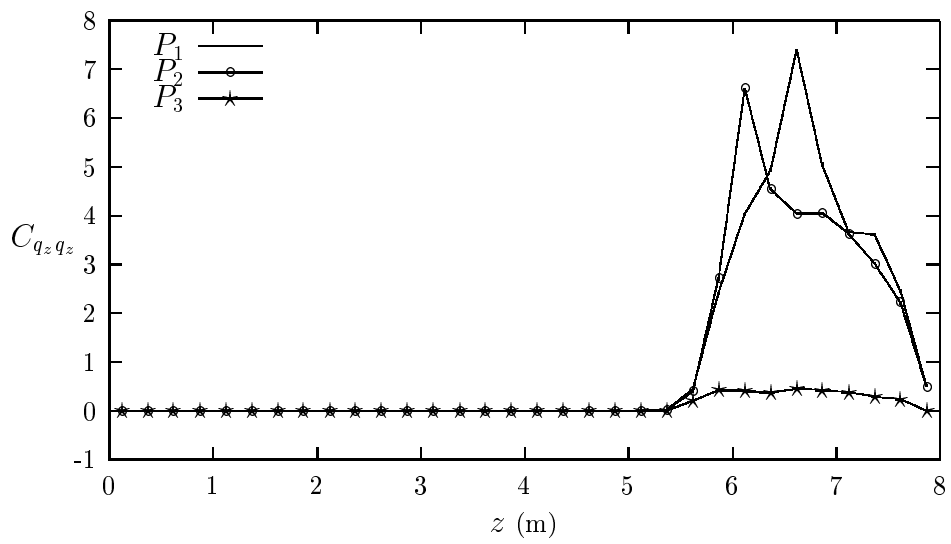


Figure 17